Heliyon 9 (2023) e15412

Contents lists available at ScienceDirect

Heliyon

journal homepage: www.cell.com/heliyon

Research article

Mathematical modelling and simulation of leak detection system in crude oil pipeline

Wasiu Yussuf Oseni [a], Olubukola Adebowale Akangbe [b,*], Kingsley Abhulimen [a]

[a] University of Lagos, Department of Chemical and Petroleum Engineering, Akoka, Yaba Lagos, Nigeria
[b] École Spéciale de Mécanique et d'Electricité (ESME Sudria), Paris, 94200, France

ARTICLE INFO

Keywords:
Emergency preparedness
Environmental safety
Crude oil pipeline
Finite difference
Leak detection
Numerical simulation

ABSTRACT

A first-order differential leak detection model that accurately detects leaks in a crude oil pipeline is presented. This model incorporates a leak factor K_L in the axial direction, which is simulated by applying the finite element method of numerical solution using COMSOL multi-physics software. Additionally, the model includes the transport equation for turbulent kinetic energy and the rate of kinetic energy model. Eigenvalues for velocities and pressures were determined and plotted against time for various pipe segments. The system is stable when the Eigenvalue is zero, but a leak is declared when the Eigenvalue for pressure or velocity is less than one. The study shows that pressure measurements are more sensitive parameters for detecting leaks than velocity measurements, and the sinusoidal waveform characterizes leak behaviours for velocity.

1. Introduction

Crude oil and gas from the reservoir and wellbore need to be transported to the separators, treaters, and storage tanks for treatment, processing, and storage before being made available to customers. One way of achieving this is through pipelines, as oil and gas pipeline systems have been proven to be the most economical and safest means of transporting petroleum, providing the highest level of reliability and efficiency [1]. However, failure sometimes occurs in a pipeline. This could be due to one or several factors, including corrosion of the pipe wall and pipeline vandalism [2].

Leakages of transported energy result in environmental pollution, economic losses, wasted energy, and a waste of resources. The effect of pipeline leakages in densely populated areas is more serious and could constitute a major threat to human lives and property [2,3]. Over the past 30 years, pipeline leakages have resulted in more than 500 deaths, thousands of injuries, and roughly $7 billion in losses. These accidents have had a significant impact on both individuals and the economy [4]. Therefore, it's essential for a pipeline system to have a quick and accurate leak awareness scheme.

Several leak detection models have been proposed by different authors. However, most of them have performed below expectations according to the criteria of robustness, cost, accuracy, response time, sensitivity, and reliability set out in the American Petroleum Institute (API) performance requirement guidelines [5[6,7]]. There are acoustic emission-based leak detection methods in pipeline [8, 9]. The results of a study that investigated pipeline failure experimentally around the socket joint using acoustic emission and pattern recognition show that acoustic emission-based methods of pipeline leak detection can exhibit high sensitivity over long distances.

* Corresponding author.
E-mail addresses: wasiuoseni.w@gmail.com (W.Y. Oseni), olubukola.akangbe@esme.fr (O.A. Akangbe), kabhulimen@unilag.edu.ng (K. Abhulimen).

https://doi.org/10.1016/j.heliyon.2023.e15412
Received 12 September 2022; Received in revised form 2 April 2023; Accepted 6 April 2023
Available online 14 April 2023

Nomenclature

Symbol	*Description*
C_μ	Adjustable coefficient for viscosity
σ_k	Adjustable coefficient 2
$C_{\varepsilon 1}$	Adjustable coefficient 3
$C_{\varepsilon 2}$	Adjustable coefficient 5
θ	Angle subtended by layer of fluid to the horizontal
ρ	Density of fluid
σ	Direct stress
ψ_j^e	Lagrange interpolation function of degree n-1
v	velocity of fluid in θ-direction
U	velocity of fluid in radial direction
W	Velocity of fluid in Z – direction
t	time in seconds
ε	Rate of dissipation of kinetic energy
τ	Shear stress
$\overline{v}$	Time average velocity
μ	viscosity of fluid
x_i^e	Global coordinate of the ith node of element Ω^e
Z	Pipe distance in axial direction
r	Radius of the pipe
p	Pressure of fluid
g_z	Component of gravitational acceleration
T	Time period average
K	Turbulent kinetic energy/m

Additional strategies, such as pipeline pressure amplification, may be necessary to supplement noise-increasing measures to address leakage [10].

Also, an electromechanical impedance-based method is available. One of the major advantages of using this method is its ability to utilize a single piezoelectric transducer to act as both a sensor and an actuator. However, due to lower Curie temperatures, it is very difficult to apply this approach at high temperatures [11]. The mass balance compensation method can perform well in various pipeline systems under different operating conditions, but a major issue with this model is that it is sensitive to random disturbances and the dynamics of pipelines, and it is unable to locate the location of leaks [12].

Capacitive sensor-based leak detection is becoming increasingly popular in the oil and gas industry for its environmental monitoring capability [12]. This method identifies a leak by measuring a change in the dielectric constant of the medium surrounding the sensor [13]. While the sensitivity of the sensor in relation to the size of the leak depends on the distance between the position of the leak and the drift of the leaking medium. However, operators have reported that this method can give false alarms because the sensor is often required to be in direct contact with the leaking medium [14].

Furthermore, a dynamic modelling-based leak detection system is employed to detect anomalies in both surface and subsea pipelines. It takes measurements from both transient and statistical points of view. Transient waves in fluid are a technique used for the detection of existing faults, features in pipelines, and different elements of the topology of the water system [15]. This model utilizes hydraulic equation with the real pipeline data to formulate hydraulic profile.

A leak is declared through continuous monitoring of transient event or noise levels. This is done by comparing measured and calculated flow, temperature, pressure, and other parameters associated with fluid transport at the inlet, outlet, or several points along the pipeline [16]. However, in addition to having complex mathematical expression, this method is also labour intensive, and

Table 1
Existing leak detection models and their operational challenges.

Leak detection Model	Challenges	Reference
Acoustic emission-based leak detection methods in pipeline	Noise due to leakages	Cramer et al. (2014)
Electromechanical impedance-based method	Inefficiency at high temperature	Zhu et al. (2019
Mass balance compensation method	Sensitivity to random disturbances, and unable to locate leak	Na et al. (2016)
Capacitive sensor-based method	False alarm is detected	Na et al. (2016), Kareem et al. (2015), Dairo et al. (2019)
Dynamic modelling -base leak detection	The model is labour intensive, and expensive to implement	Bohorquez et al. (2020)

expensive to implement [17]. The summary of different model and their operational challenges are shown in Table 1.

A new model is presented for optimal detection of leaks in crude oil pipelines. This model is cheap, fast, robust, and highly reliable, outperforming other previously discovered leak detection methods [18]. The model uses the concept of Eigenvalues of pressure and velocity to evolve a criterion for pipeline leak detection. A flow model was derived for a typical pipeline network, and the inclusion of the leak factor K_L in the model provides an indication of the relative degree of deviation from a no-leak situation. The first-order differential equations describing the flow process were solved using a numerical solution by the finite element scheme in the COMSOL multi-physics environment.

A set of parametric velocity and pressure profiles were generated and validated using industrial data. Eigen pressures and velocities were calculated from the deviation model of pressure and velocity. A leak is detected whenever any of the Eigen values is less than 1. The simulation profiles of Eigen pressure and velocity for a crude oil company in the Niger Delta region of Nigeria show that pressure deviations are more sensitive parameters for leak detection than velocity measurements.

2. Materials and methods

This study involves the formulation and presentation of a unique model that describes the flow behaviour for a pipeline leak detection system for liquids such as crude oil. The model formulation was made possible through the introduction of a leak factor, K_L, in the flow model Navier-Stokes equation of motion for cylindrical coordinates. The liquid flow motion considered is highly turbulent; therefore, kinetic energy was introduced and dissipated. Hence, the flow model was solved alongside models that describe the production and dissipation rates of turbulent kinetic energy, using the finite element method as the numerical solution method implemented in the COMSOL Multiphysics computer application software.

2.1. Modelling concept and validation

A new model for detecting leaks optimally in liquid pipelines is presented. The model utilizes the concept of eigenvalues of pressure and velocity to develop a criterion for pipeline leak detection. A flow model was derived for a typical pipeline network, and the inclusion of the leak factor K_L in the flow model provides an indication of the relative degree of deviation from a no-leak situation. The numerical solution by the finite element scheme was used to solve the first-order differential equations describing the flow process simulated in the COMSOL Multiphysics environment. Table 2 contains industry data used to validate the derived model, obtained from a leading oil and gas operator in the Niger Delta of Nigeria. Table 2(a) displays the velocity head per pipe fitting, Table 2(b) shows important data for this modelling validation known as pipe network flow data, and Table 2(c) provides pipe node segment roughness data (seeTable 3).

2.2. Model development

2.2.1. Flow model development

Fig. 1 depicts the elemental strip of the pipeline segment under consideration. The net rate of change of mass along the elemental strip is given by the differential equation (1) as shown below:

$$\left(\frac{1}{r}\frac{\partial}{\partial r}(\rho u r)+\frac{1}{r}\frac{\partial}{\partial \theta}(\rho v)+\frac{\partial}{\partial z}(\rho w)\right)+\frac{\partial}{\partial t}(\rho)=0 \tag{1}$$

where r is the coordinate of the cylinder in the radial direction in meters, θ is the coordinate of the circumferential or tangential direction in radians per second, and z is the coordinate in the axial direction in meters. ρ is the density of the fluid in kilograms per cubic meter, and u, v, and w are the velocities of the fluid in the r, θ, and w directions, respectively, in meters per second. At steady

Table 2(a)
Velocity head per pipe fitting.

Fitting or Valve	K_v, number of Velocity Heads per fitting	K_mNumber of Equivalent pipe diameters
45° Standard Elbow	0.35	15
45° Long Radius Elbow	0.2	10
90° Standard radius Elbow	0.6–0.8	30–40
90° Standard long Elbow	0.45	23
90° Standard Elbow	1.5	75
Tee –entry from Leg	1.2	60
Tee-entry into Leg	1.8	90
Union and Coupling	0.04	2
Sharp Reduction (Tank Outlet)	0.5	25
Sudden Expansion (Tank Inlet)	1.0	50
Gate Valve: Fully open	0.15	7.5
¼ Open	16	800
½ Open	4	200
¾ Open	1	40

Table 2(b)
Pipe network flow data.

Node Identity	Location	Flow 10^{-3} b/d	Water Cut	Oil S. G	Oil Visc	Velo m/s	Flow Regime	Liquid Hold Up	Node Pres Bar
(0,0,0)	M1	189.36	0.578	0.8753	5.225	1.19	0.17Emul	1	3.5
(0,0,1)	M1	189.36	0.578	0.8753	5.233	1.19	0.17Emul	1	13.5
(0,0,2)	M2	168.36	0.588	0.8759	4.97	1.06	0.13Emul	1	13.5
(0,0,3)	M3	127.91	0.643	0.3937	7.423	1.16	Oil in water	1	15.1
(0,0,4)	M4	52.85	0.545	0.829	7.564	0.48	Water in Oil	1	18.5
(0,0,5)	M5	52.85	0.545	0.829	7.579	0.75	0.02Emul	1	18.5

Table 2(c)
Pipe node segment roughness data.

Node Identity	Location	Elevation	Length	Pipeline ID (in)	Segment Roughness
(0,0,0)	M1	0	45870	24.00	0.0499
(0,0,1)	M2	0	0	24.00	0.0499
(0,0,2)	M3	0	9450	24.0	0.0499
(0,0,3)	M4	0	18970	20.0	0.0499
(0,0,4)	M5	0	0	16.0	0.0499
(0,0,5)	M6	0	16640	16.0	0.0499
(0,0,6)	M7	0	17050	16.0	0.0499

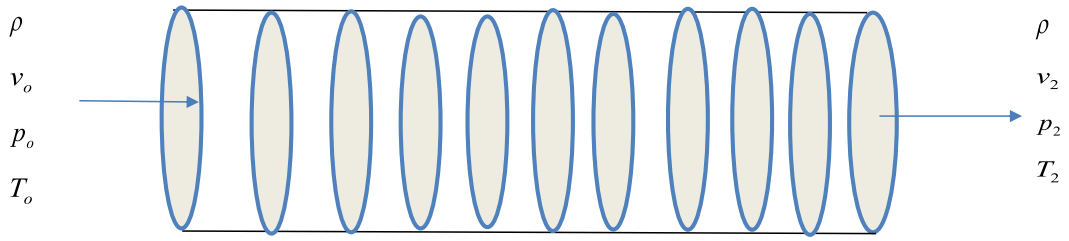

Fig. 1. The elemental strip of the modelled pipeline segment.

state, the net rate of change of mass along the elemental strip element becomes:

$$\left(\frac{1}{r}\frac{\partial}{\partial r}(\rho ur)+\frac{1}{r}\frac{\partial}{\partial \theta}(\rho v)+\frac{\partial}{\partial z}(\rho w)\right)=0 \tag{2}$$

Assuming the flow in pipe in the axial direction only is considered, therefore neglecting the forces in r and Θ directions, the net force (Fz) in the axial (z) direction is derived as.

$$F_z=\left(\frac{\partial}{\partial r}r\tau_{rz}+\frac{\partial}{\partial \theta}\tau_{\theta z}+\frac{\partial}{\partial z}r\sigma_{zz}\right)\Delta r\Delta\theta\Delta z \tag{3}$$

where F_z is the axial directional force, and τ_{rz}, $\tau_{\theta z}$, τ_{zz} are the shear stresses, and axial stress in N/m2

Since pressure decreases in the direction of fluid flow, the net pressure force in

Axial (z) direction is given by.

$$P_z=-\frac{\partial p}{\partial z}\Delta\theta\Delta r\Delta z \tag{4}$$

Momentum flow into and out of the phase of the elemental pipe segment is by both convection (bulk flow) and molecular transfer (velocity gradients). Here the bulk flow is in r-phase while Molecular transfer occurs in the θ and z phases. The velocity in the r, θ, and z phases is denoted by u, v, and w respectively. Furthermore, we are neglecting the net momentum in the r and θ directions since we are assuming fluid flow only in the z direction.

The net z momentum is given from the differential model below.

$$MM_z=-\left(\frac{\partial}{\partial r}(\rho uwr)+\frac{\partial}{\partial \theta}(\rho vw)+\frac{\partial}{\partial z}(\rho wwr)\right)\Delta z\Delta\theta\Delta r \tag{5}$$

The net rate of change of momentum within the elemental pipe segment, and r is not changing with the position in z-direction is

given as.

$$M_t = r\frac{\partial}{\partial z}(\rho w)\Delta\theta\Delta z\Delta r \tag{6}$$

where MMZ is the net z-momentum in kgm/s, and Mt is the net rate of change of momentum in z-direction in kgm/s.

The component of gravitational force Gz in axial z direction is given by as.

$$G_z = \rho g_z\ \Delta r\Delta\theta\Delta z \tag{7}$$

with the Gz, the component of the axial gravitational force, gz is the acceleration due to gravity along the axial direction.

Applying the first law of motion in axial direction on the elemental pipe segment to determine the flow model in z-direction for the elemental pipe segment.

(Rate of change of momentum) = (momentum addition across the surface) + (the net pressure force) + (gravitational force) + (net surface force) as indicated in equation (8) shown below

$$\rho\left(\frac{\partial w}{\partial t}+u\frac{\partial w}{\partial r}+\frac{v}{r}\frac{\partial}{\partial\theta}w+w\frac{\partial w}{\partial z}\right)-\frac{\partial p}{\partial z}+\frac{1}{r}\frac{\partial}{\partial r}r\tau_{rz}+\frac{1}{r}\frac{\partial}{\partial\theta}\tau_{\theta z}+\frac{\partial}{\partial z}\sigma_{zz}+\rho g_z=0 \tag{8}$$

2.2.2. The flow behaviour of liquid pipeline system

This model was derived by the introduction of a leak factor KL which accounts for any leakage disturbances in the flow liquid within the pipeline system.

By incorporating the leak factor into the flow model (equation (8)), which represents the innovative leak detection system's model.

$$\rho(1+K_L)\left(\frac{\partial w}{\partial t}+u\frac{\partial w}{\partial r}+\frac{v}{r}\frac{\partial}{\partial\theta}\rho w+w\frac{\partial w}{\partial z}\right)=-\frac{\partial p}{\partial z}+\frac{1}{r}\frac{\partial}{\partial r}r\tau_{rz}+\frac{1}{r}\frac{\partial}{\partial\theta}\tau_{\theta z}+\frac{\partial}{\partial z}\sigma_{zz}+\rho g_z \tag{9}$$

Equation (9) represents the model developed for the leak detection system, which is a first-order differential equation. This leak detection model was solved using the finite element method and simulated in the COMSOL multi-physics software environment, along with transport equations for turbulent kinetic energy and the rate of dissipation of kinetic energy.

The transport model for the turbulent kinetic energy is given as.

$$\rho\frac{\partial k}{\partial t}+\rho\overline{v}\cdot\nabla k=\nabla\cdot\left[\left(\mu+\rho\frac{C_\mu k^2}{\sigma_k\varepsilon}\right)\nabla k\right]+\rho C_\mu\frac{k^2}{\varepsilon}\left(\nabla\overline{v}+(\nabla\overline{v})^T\right)^2-\rho\varepsilon \tag{10}$$

The first term on the right-hand side (RHS) of equation (10) represents the transport of turbulence kinetic energy by pressure, viscous stresses, and Reynolds stresses, respectively. The second term represents the rate of dissipation of turbulence kinetic energy, and the last term represents turbulence production.

The rate of dissipation of kinetic energy equation is given as.

$$\rho\frac{\partial k}{\partial t}+\rho\overline{v}\cdot\nabla\varepsilon=\nabla\cdot\left[\left(\mu+\rho\frac{C_\mu k^2}{\sigma_\varepsilon\varepsilon}\right)\nabla\varepsilon\right]+\rho C_{\varepsilon1}C_\mu k\left(\nabla\overline{v}+(\nabla\overline{v})^T\right)^2-\rho C_{\varepsilon2}\frac{\varepsilon^2}{k} \tag{11}$$

The following boundary conditions were use at the inlet U o = 0, V o = 0, W o = 119, and outlet Po = 0, and the logarithmic wall condition.

2.2.3. Computations of leak hole diameters, deviation pressures and velocities

For lines transporting single-phase liquids from one pressure vessel to another by pressure differential, the flow velocity should not exceed 15 feet/second at the maximum flow rate to minimize flashing ahead of the control valve. In practice, the flow velocity should not be less than 3 feet/second to minimize the deposition of sand and other solids. At these flow velocities, the overall pressure drop in the piping will usually be small. Most of the pressure drop in liquid lines between two pressure vessels will occur in the dump valve and/or choke. API 14E states that flow velocities in liquid lines can be calculated using the following derived equation.

$$v=\frac{0.012Q}{D^2} \tag{12}$$

where Q is the flow rate in cubic feet per second, and D is the diameter of the cylindrical pipe in feet.

Erosional velocity, which is the velocity above which erosion may occur, is given as:

$$v_e=\frac{c}{\sqrt{\rho}} \tag{13}$$

where *Ve* is the fluid erosional velocity in ft/s, *c* is the empirical constant in $\sqrt{(lb/(ft\bullet s\hat{}2))}$, and ρm is the gas/liquid mixture density at the flowing pressure and temperature in lb/ft^3.

It is important to note that the inside diameter will be sufficient to accommodate the flowing liquid flow rate only if the fluid

velocity is lower than the fluid's erosional velocity. Based on the theory outlined above, the diameter of the leak hole is given as:

$$D_L = \sqrt{\frac{0.012 Q_L}{v_L}} \tag{14}$$

where D_L is the leak diameter in ft, Q_L is the leak volumetric flowrate in ft/s, V_L is the velocity at the leak location.

At leak point, QL is assumed a value equal to

$Q_L = Q_1 - Q_2$ where QL is the volume of leakage, Q1 is the inlet crude volumetric flowrate, and Q2 is the outlet volumetric flowrate.

$$\mathrm{Q2} = \mathrm{Q1}\ (1 - \mathrm{KL}) \tag{15}$$

where KL is the leak detection factor.

The Eigen models for pressure is written as shown in Equation 16

$$p_n = \frac{p_{i+2,j} - p_{i+1,j}}{p_{i+1,j} - p_{ij}} \tag{16}$$

The Eigen Model for velocity is written as shown in Equation (17) below.

$$v_n = \frac{v_{i+2,j} - v_{i+1,j}}{v_{i+1,j} - v_{ij}} \tag{17}$$

2.2.4. Finite element model

The finite element model is obtained from the approximate solution of the form.

$$u \approx U^e = \sum_{j=1}^{n} u_j{}^e \psi_j{}^e(x) \tag{18}$$

where $\psi_j{}^e$ is the Lagrange interpolation function of degree n-1

$$0 = \int_{x_A}^{x_B} \left(a \frac{dw}{dx} \frac{du}{dx} + cwu \right) dx - \int_{x_A}^{x_B} wq dx - \sum_{i=1}^{n} w(x_i{}^e) Q_i{}^e \tag{19}$$

where $x_i{}^e$ is the global coordinate of the ith node of element Ω^e.

The n algebraic expressions are obtained from Equation (17) and Equation (18) which gives the form of Equation (20) as shown below:

$$\begin{aligned}
0 &= \int_{x_A}^{x_B} \left[a \frac{d\psi_1^e}{dx} \left(\sum_{j=1}^{n} u_j{}^e \frac{d\psi_1^e}{dx} \right) + c\psi_1^e \left(\sum_{j=1}^{n} u_j{}^e \psi_1^e(x) \right) - \psi_1^e q \right] dx - \sum_{j=1}^{n} \psi_1^e(x_j{}^e) Q_j{}^e \\
0 &= \int_{x_A}^{x_B} \left[a \frac{d\psi_2^e}{dx} \left(\sum_{j=1}^{n} u_j{}^e \frac{d\psi_2^e}{dx} \right) + c\psi_2^e \left(\sum_{j=1}^{n} u_j{}^e \psi_2^e(x) \right) - \psi_2^e q \right] dx - \sum_{j=1}^{n} \psi_2^e(x_j{}^e) Q_j{}^e \\
&\vdots \\
0 &= \int_{x_A}^{x_B} \left[a \frac{d\psi_n^e}{dx} \left(\sum_{j=1}^{n} u_j{}^e \frac{d\psi_j^e}{dx} \right) + c\psi_n^e \left(\sum_{j=1}^{n} u_j{}^e \psi_j^e(x) \right) - \psi_2^e q \right] dx - \sum_{j=1}^{n} \psi_n^e(x_j{}^e) Q_j{}^e
\end{aligned} \tag{20}$$

The ith algebraic equations can be written as

$$0 = \sum_{j=1}^{n} K_{ij}{}^e u_j{}^e - f_i{}^e - Q_i{}^e \quad (i = 1, 2, \ldots\ldots, n). \tag{21}$$

where

$$\begin{aligned}
k_{ij}{}^e &= \int_{x_A}^{x_B} \left(a \frac{d\psi_i^e}{dx} \frac{d\psi_j^e}{dx} + c\psi_i{}^e \psi_j{}^e \right) dx = B\left(\psi_i^e, \psi_j^e\right), \\
f^e &= \int_{x_A}^{x_B} q\psi_i^e dx = l\left(\psi_i^e\right) \\
Q_i{}^e &= \sum_{j=1}^{n} \psi_j^e(x_i{}^e) Q_j{}^e = Q_i{}^e
\end{aligned} \tag{22}$$

Therefore,

$$[K^e]\{u^e\} = \{f^e\} + \{Q^e\}$$

The connectivity of the element can be gotten from Equation (23) below.

$$\sum_{j=1}^{n}\left(K_{nj}{}^{e}u_j{}^{e} + K_{1j}{}^{e+1}u_j{}^{e+1}\right) = f_n{}^{e} + f_1{}^{e+1} + \left(Q_n{}^{e} + Q_1{}^{e+1}\right) = f_n{}^{e} + f_1{}^{e+1} + Q_0 \tag{23}$$

3. Results and discussion

3.1. Technicalities of the pressure and velocity profiles along pipeline segments

Fig. 2[(a)-(f)] show velocities across different pipeline segments, and Fig. 3[(a)-(f)] show the pressure profile along the pipeline segments. It was observed that there was an increase in velocity along the pipeline segments. The pipeline segments in Fig. 2(a) with $K_L = 0$, 0.29018, 0.4305, 0.527, and 0.6550 indicate that as the leak factor increases, the velocity profile increases along the length of the pipe. Additionally, it can be observed that in Fig. 2(b), the velocity profile starts from 0 and increases as the leak factor increases along the length of the pipe. The velocity profile is reduced at 9 m along the pipe length, indicating the leak location. Above 9 m, the velocity profile continues to increase with an increase in the leak factor. The loss of pressure between the inlet and outlet is an indication of

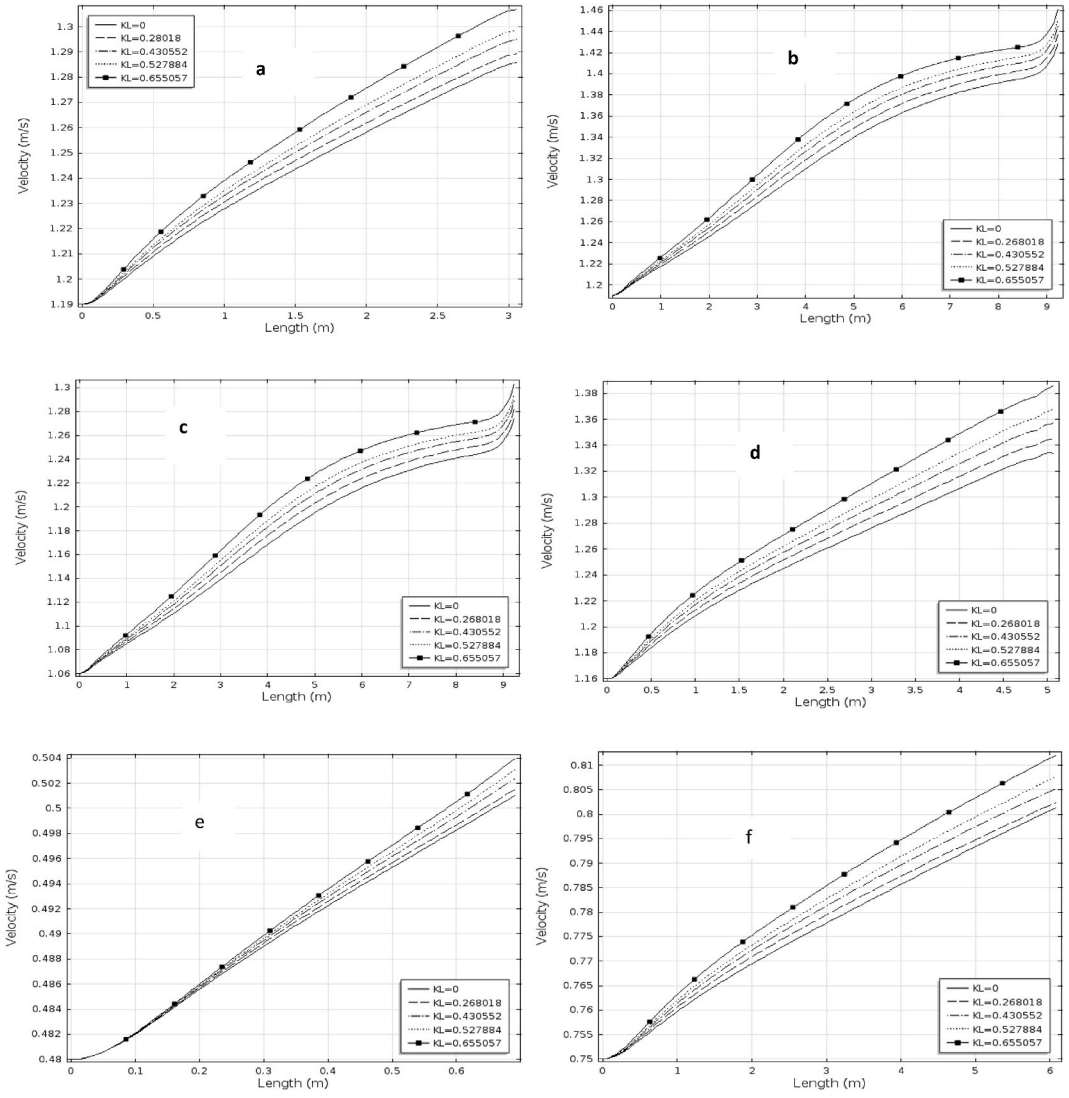

Fig. 2. Velocity profiles along pipeline segments: (a)Segment 1(b) Segment 2 (c) Segment 3 (d) Segment 4 (e) Segment 5 (f) Segment 6.

leakage in a pipeline, and a large drop in pressure values indicates a leakage in the pipeline system [19]).

In Fig. 3(a), the pressure profile decreases as the leak factor increases along the pipeline distance, and it is linearly proportional to the distance along the pipeline segment under consideration. In Fig. 3(b), the pressure profile behaves in the same way as that of Fig. 3 (a) as the leak factor increases along the pipeline distance. Overall, the pressure is linearly proportional to the distance, as observed from Fig. 3[(a)–(f)]. This result indicates that the pressure profile measurements along the pipeline segment show a waveform and quantitative dynamic behaviour when leakages are experienced in the pipeline segment.

3.2. Eigen velocity and pressure profile along the pipeline segments

Fig. 4[(a)-(f)] show the Eigen velocity along the different pipeline segments under consideration, and Fig. 5[(a)-(f)] depict Eigen pressure along the same pipeline segment for this study. In Fig. 4(a), a negative Eigen value was observed between 1.568min and 1.575min, which indicates a leak scenario. The minimum Eigenvalue velocity was attained at −75 and 1.575min. A surge was then noticed between 1.575min and 1.58min with normal flow between 1.58min and 1.588min. After 1.588min, another surge was noticed, and at 1.59min, a leak was observed. On the other hand, Fig. 5(a) showed that the Eigen pressure value decreases within the first 0.5 min and later becomes constant above this time, which also depicts a surge scenario. In Fig. 4(b), the simulation result between 6.23min and 6.33min indicates a leak scenario being mimicked, attaining a minimum Eigenvalue velocity at −150 and 6.3min. Then, a

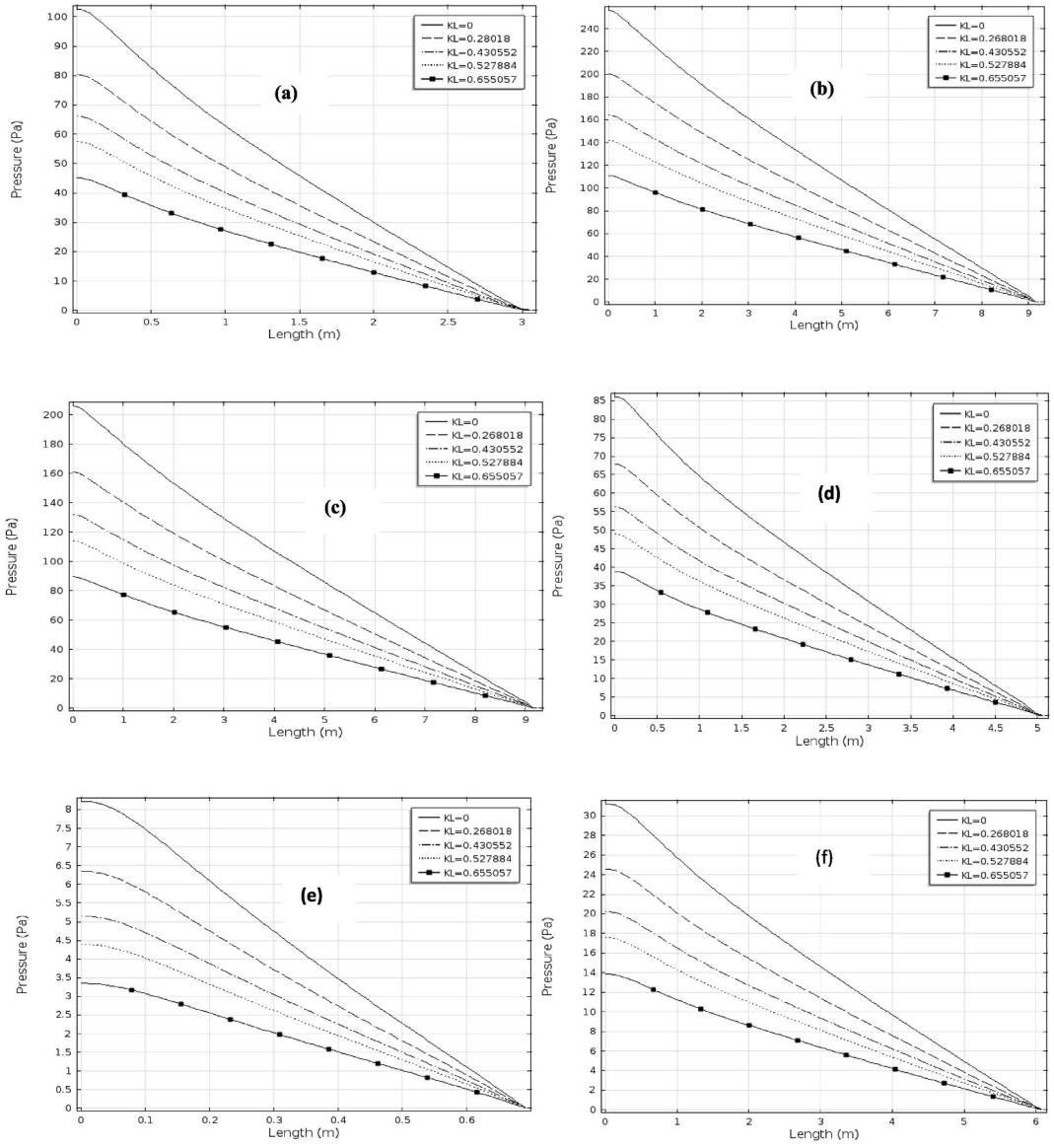

Fig. 3. Pressure profiles along pipeline segment: (a)Segment 1 (b) Segment 2 (c)Segment 3 (d)Segment 4 (e) Segment 5 (f) Segment 6.

surge is noticed between 6.33min and 6.335min with normal flow between 6.35min and 6.4min.

Fig. 5(b), however, showed that the Eigen pressure value decreases within the first 2 min and later becomes constant above this time, which depicts a surge scenario. Fig. 4(c) simulated result indicates negative values between 7.0 min and 7.16 min, which implies a leak scenario, attaining a minimum eigenvalue velocity at −45 and 7.14 min. It was noticed that normal flow was present between 7.16 min and 7.2 min, and between 7.2 min and 7.25 min. Fig. 5(c) showed that the Eigen pressure value decreases within the first 2 min and later becomes constant above this time, eventually tending towards a surge scenario.

Fig. 4(d) depicts the negative portion between 3.71 min and 3.739 min, which indicates a leak scenario. Then, attaining a minimum eigenvalue velocity at −1 and 3.71 min, with a surge being noticed between 3.74 min and 3.769 min, and normal flow being observed between 3.769 min and 3.77 min. Fig. 5(d) showed that the Eigen pressure value decreases within the first 0.5 min and later becomes constant above this time, depicting a surge scenario.

The waveform of Fig. 4(e) is also in the negative portion between 1.373 min and 1.377 min, indicating a leak scenario by attaining a minimum eigenvalue velocity at −175 and 1.375 min. A surge is noticed between 1.377 min and 1.379 min, with normal flow present above 1.379 min. Fig. 5(e), however, showed that the Eigen pressure value decreases within the first 0.1 min and later becomes constant above this time, which depicts a surge scenario.

The waveform of Fig. 5(e) is in the negative portion between 7.49 min and 7.56 min, indicating a leak scenario by attaining a minimum eigenvalue velocity at −78 and 7.53 min. A surge is noticed between 7.56 min and 7.58 min, followed by a momentary normal flow at 7.59 min, and finally a surge above 7.59 min. Fig. 5(f), however, showed that the Eigen pressure value decreases within the first 2 min and later becomes constant above this time, which depicts a surge scenario as well.

According to Abhulimen et al. [20], the waveform equilibrates from an unsteady to a steady situation, which is characterized by trends in the eigen pressure values with pipeline distance under different leak factor conditions. The relative amount of eigen velocity plots would be negative, which indicates that eigen velocity alone is not sufficient to correlate a leak. On the other hand, the pressure profile of the eigenvalues is greater than the negative eigenvalues experienced in the case of eigen velocity [20]. Therefore, the pressure profile would be a better index for leak location and identification [21].

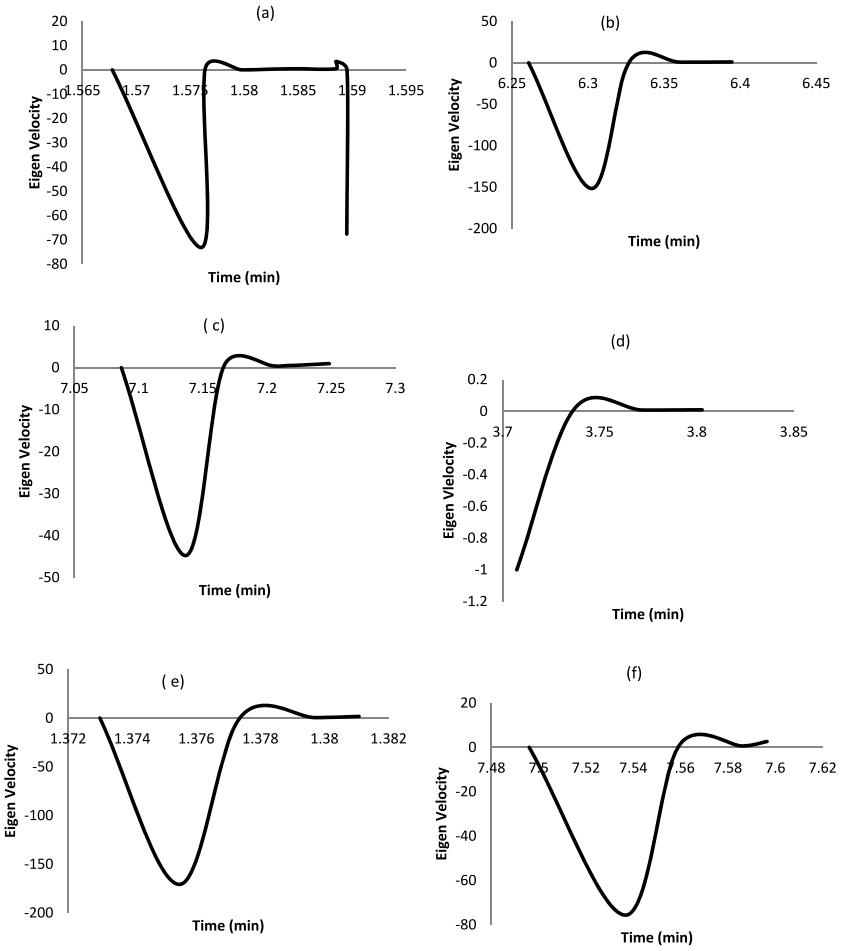

Fig. 4. Eigen Velocity of Pipeline segment along: (a) Segment 1 (b) Segment 2 (c) Segment 3 (d) Segment 4 (e) Segment 5 (f) Segment 6.

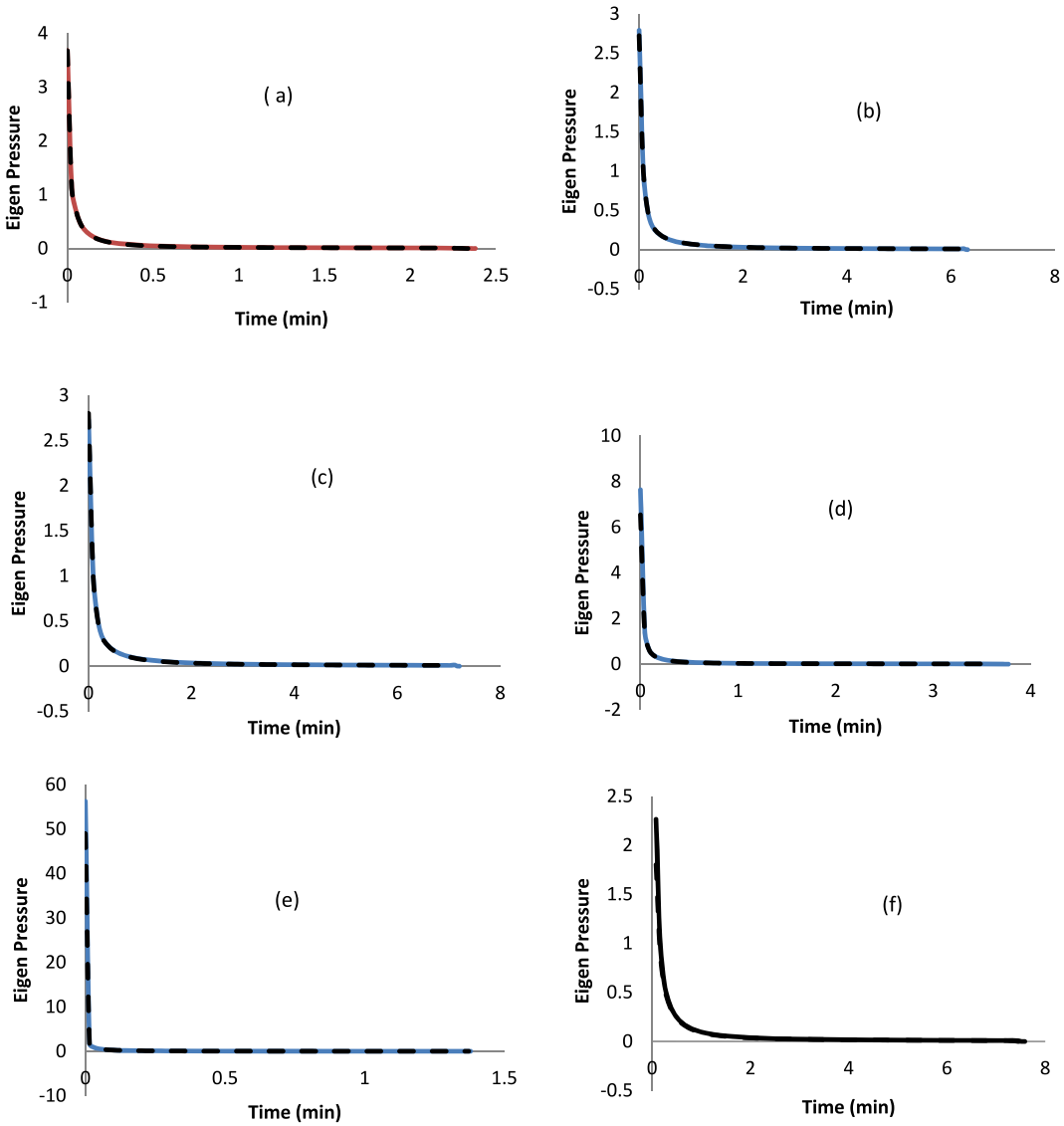

Fig. 5. Eigen pressure profile along pipeline Segment: (a) Segment 1 (b) Segment 2 (c)Segment 3 (d) segment 4 (e) Segment 5 (f) Segment 6.

3.3. Diameter of leak holes in the pipeline segment

Table 3[(a)–(e)] shows the effects of the leak factor on the pipeline leak hole diameter. As depicted in Table 3(a), the leak volumetric flow rate increases by 97% as the leak factor increases from 0.018644 to 0.6551, while the pipeline leak hole diameter increases from 3.291 inches to 19.53 inches. In Fig. 3(b), the leak hole diameter increases from 2.74 inches to 16.24 inches, and the increase in leak volumetric flow rate is almost as high as what was obtained in Table 3(a). Across all pipeline segments considered, pipeline leak hole diameter increases with an increase in the leak factor. The actual volumetric flow rate of leakages also increases as the leak factor increases, as shown by the results.

3.4. model field testing strategy

For nearly all subsea oil and gas pipelines, the operational flow regimes are highly turbulent. For leaks from pressurized subsea gas pipelines, it can be safely assumed that the leak will act as a sound source. However, for static heavy oil lines, it is possible that the leak will not act as a sound source. In cases like this, sound is naturally imposed on the pipeline system, and variations in the wave generated will be detected as an anomaly, which can indicate an intrusion or a leak. A leak factor, K_L, is calculated. The presence of a leak is manifested by an increased noise level. There are many potential reasons for an increased noise level, and considerable further

Table 3(a)
Diameter of leak hole for Pipeline Segment 1 and 2.

Leak factor (K_L)	Pipe diameter (D)in inches	Leak volumetric flow rate (Q_L) in barrels/day	Pipeline Leak hole diameter (D_L) in inches	Outlet crude volumetric flow rate (Q_2) in barrels/day	inlet crude volumetric flow rate (Q_1) in barrels/day	Velocity of crude (v) in feet/second
0.018644	16	3530.428	3.295885	185829.6	189360	3.9
0.108687	16	20580.97	7.957767	168779	189360	3.9
0.113258	16	21446.53	8.123382	167913.5	189360	3.9
0.268018	16	50751.89	12.49639	138608.1	189360	3.9
0.335629	16	63554.71	13.98402	125805.3	189360	3.9
0.392866	16	74393.11	15.1295	114966.9	189360	3.9
0.430052	16	81434.65	15.82934	107925.4	189360	3.9
0.509448	16	96469.07	17.22869	92890.93	189360	3.9
0.527864	16	99956.33	17.53733	89403.67	189360	3.9
0.655057	16	124041.6	19.53629	65318.41	189360	3.9

Table 3(b)
Diameter of leak hole for pipeline segment 3.

Leak factor (K_L)	Pipe diameter (D)in inches	Leak volumetric flow rate (Q_L) in barrels/day	Pipeline Leak hole diameter (D_L) in inches	Outlet crude volumetric flow rate (Q_2) in barrels/day	Inlet crude volumetric flow rate (Q_1) in barrels/day	Velocity of crude (v) in feet/second
0.018644	16	2384.754	2.740627	125525.2	127910	3.81
0.108687	16	13902.15	6.617123	114007.8	127910	3.81
0.113258	16	14486.83	6.754836	113423.2	127910	3.81
0.268018	16	34282.18	10.39112	93627.82	127910	3.81
0.335629	16	42930.31	11.62814	84979.69	127910	3.81
0.392866	16	50251.49	12.58064	77658.51	127910	3.81
0.430052	16	55007.95	13.16258	72902.05	127910	3.81
0.509448	16	65163.49	14.32618	62746.51	127910	3.81
0.527864	16	67519.08	14.58282	60390.92	127910	3.81
0.655057	16	83788.34	16.24501	44121.66	127910	3.81

Table 3(c)
Diameter of leak hole for pipeline segment 4.

Leak factor (K_L)	Pipe diameter (D)in inches	Leak volumetric flow rate (Q_L) in barrels/day	Pipeline Leak hole diameter (D_L) in inches	Outlet crude volumetric flow rate (Q_2) in barrels/day	Inlet crude volumetric flow rate (Q_1) in barrels/day	Velocity of crude (v) in feet/second
0.018644	16	3138.904	3.289955	165221.1	168360	3.48
0.108687	16	18298.54	7.943452	150061.5	168360	3.48
0.113258	16	19068.12	8.108769	149291.9	168360	3.48
0.268018	16	45123.51	12.47391	123236.5	168360	3.48
0.335629	16	56506.5	13.95887	111853.5	168360	3.48
0.392866	16	66142.92	15.10229	102217.1	168360	3.48
0.430052	16	72403.55	15.80087	95956.45	168360	3.48
0.509448	16	85770.67	17.1977	82589.33	168360	3.48
0.527864	16	88871.18	17.50578	79488.82	168360	3.48
0.655057	16	110285.4	19.50114	58074.6	168360	3.48

Table 3(d)
Diameter of leak hole for pipeline segment 5.

Leak factor (K_L)	Pipe diameter (D)in inches	Leak volumetric flow rate (Q_L) in barrels/day	Pipeline Leak hole diameter (D_L) in inches	Outlet crude volumetric flow rate (Q_2)in barrels/day	Outlet crude volumetric flow rate (Q_2)in barrels/day	Velocity of crude (v) in feet/second
0.018644	16	2384.754	2.740627	125525.2	127910	3.81
0.108687	16	13902.15	6.617123	114007.8	127910	3.81
0.113258	16	14486.83	6.754836	113423.2	127910	3.81
0.268018	16	34282.18	10.39112	93627.82	127910	3.81
0.335629	16	42930.31	11.62814	84979.69	127910	3.81
0.392866	16	50251.49	12.58064	77658.51	127910	3.81
0.430052	16	55007.95	13.16258	72902.05	127910	3.81
0.509448	16	65163.49	14.32618	62746.51	127910	3.81
0.527864	16	67519.08	14.58282	60390.92	127910	3.81
0.655057	16	83788.34	16.24501	44121.66	127910	3.81

Table 3(e)
Diameter of leak hole for pipeline segment 6.

Leak factor (K_L)	Pipe diameter (D)in inches	Leak volumetric flow rate (Q_L) in barrels/day	Pipeline Leak hole diameter (D_L) in inches	Outlet crude volumetric flow rate (Q_2)in barrels/day	Outlet crude volumetric flow rate (Q_2)in barrels/day	Velocity of crude (v) in feet/second
0.018644	12	985.3354	2.744308	51864.66	52850	1.57
0.108687	12	5744.108	6.62601	47105.89	52850	1.57
0.113258	12	5985.685	6.763909	46864.31	52850	1.57
0.268018	12	14164.75	10.40508	38685.25	52850	1.57
0.335629	12	17737.99	11.64375	35112.01	52850	1.57
0.392866	12	20762.97	12.59753	32087.03	52850	1.57
0.430052	12	22728.25	13.18025	30121.75	52850	1.57
0.509448	12	26924.33	14.34542	25925.67	52850	1.57
0.527864	12	27897.61	14.6024	24952.39	52850	1.57
0.655057	12	34619.76	16.26683	18230.24	52850	1.57

discrimination would be required before a leak could be declared, and for these reasons, disturbances are considered in the factor.

When a leak occurs in a pipeline system, a pressure wave will propagate through the pipeline upstream and downstream relative to the leak position, as shown in Fig. 6. Pipeline leaks can be detected by observing the external effects of the spill or by monitoring and analysing the internal hydraulics of the pipeline system, as shown in Fig. 6. The detection and analysis of pressure transients generated by a leak occurrence, together with the measured wave velocity, allow the detection and location of leaks in pipelines. Fig. 7(b) shows the evolution of the hydraulic volume of the gas leak and the leak detection factor. The level of noise produced to alert the leak occurrence depends on the leak detection factor shown in Fig. 7(a) and the hydraulic volumetric leakage, as observed in Fig. 7(b).

3.5. Future prospect

In this study, the leak detection model was derived and simulated in only one dimension. The choice of one dimension was made to keep the mathematical concept simple and to provide insight into the fundamental principles of leak detection systems. However, it is crucial to address the aspects of leak detection in two and three dimensions, which represent the actual real system, in future work.

Moreover, to consider and broaden the application of the proposed method to more complex scenarios, such as multiple leaks in crude pipeline networks, experimental tests should be conducted to verify the application of this method.

4. Conclusions

The leak factor K_L in the axial direction has been developed and simulated in the COMSOL Multi-physics software environment, along with transport equations for the turbulent kinetic energy model and the rate of dissipation of kinetic energy model. The study has led to the following conclusions.

1. The pressure profile decreases sharply as leak factor increases along the pipeline distance.
2. The velocity profile increases as leak factor increases along the pipeline distance.

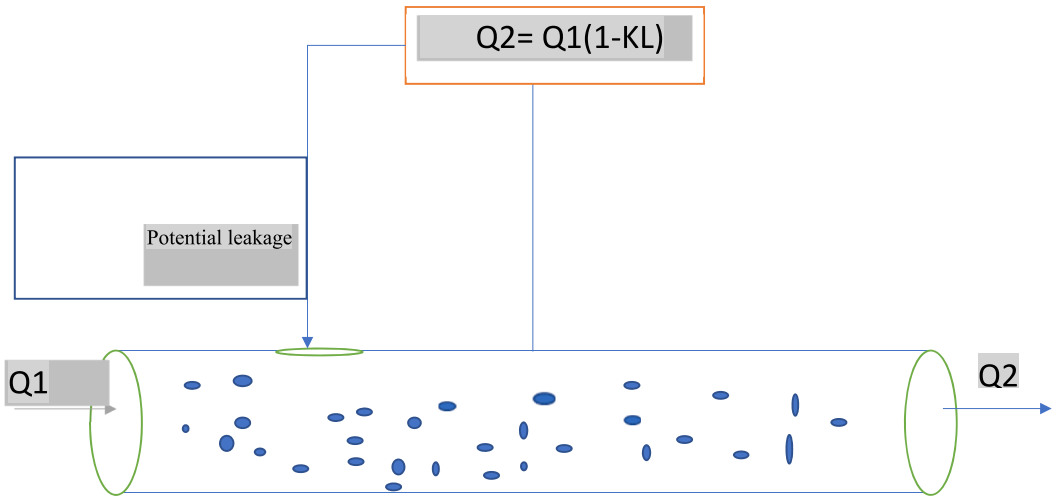

Fig. 6. Flow configuration with leak detection factor along pipeline carrying crude oil.

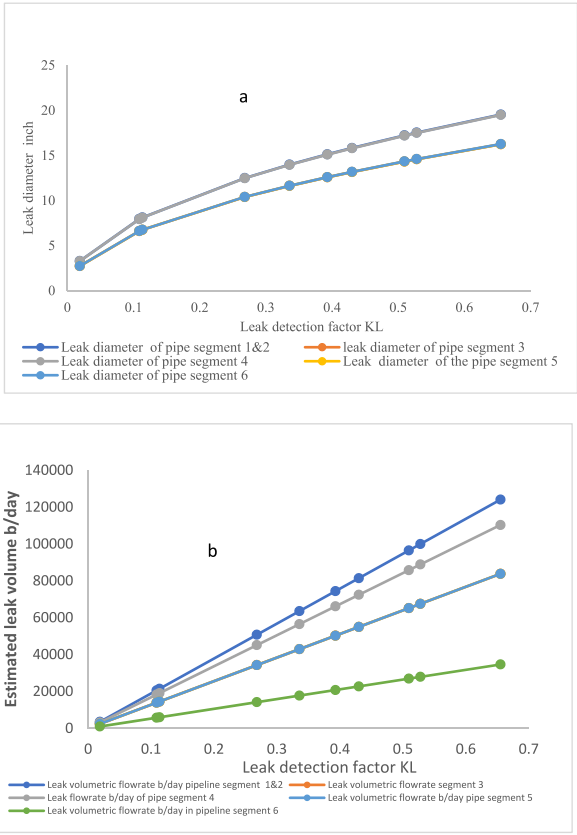

Fig. 7. Performance characterization of leak detection system: (a) Leak size variation with leak detection factor (b) Leak volume variation with leak detection factor.

3. Sinusoidal waveform characterizes leak and surge behaviours for velocity measurements, whereas decay curves characterize surge behaviours for pressure measurements.
4. Due to sharp drop in the pressure profiles, pressure measurements are more sensitive parameters for leak detection than velocity measurements.

Author contribution statement

Olubukola Adebowale Akangbe: Conceived and designed the experiments; Analysed and interpreted the data; Wrote the paper. Wasiu Yusuff Oseni: Conceived and designed the experiments; Performed the experiments; Analysed and interpreted the data; Wrote the paper. Kingsley Abhulimen: Conceived and designed the experiments; Analysed and interpreted the data; Contributed reagents, materials, analysis tools or data; Wrote the paper.

Funding statement

This research did not receive any specific grant from funding agencies in the public, commercial, or not-for-profit sectors.

Data availability statement

Data will be made available on request.

Declaration of competing interest

The authors declare that they have no known competing financial interests or personal relationships that could have appeared to influence the work reported in this paper.

References

[1] Q. Xiao, J. Li, H. Feng, S. Jin, Natural-gas pipeline leak location using vibrational mode of decomposition analysis and cross time frequency spectrum, Measurement 124 (2018) 163–172 ([CrossRef]).

[2] L. Ajao, E. Adedokun, C. Nwishieyi, M. Adegboye, J. Agalo, J. Kolo, An anti-theft oil pipeline vandalism detection:embedded system development, Int. J. Eng. Sci. Appl. 2 (2) (2018) 55–64 ([CrossRef]).

[3] M. Yu, S. Wan, K. Zheng, P. Guo, T. Chu, Z. Yuan, Influence on the methane/air explosion characteristics of the side venting position in a pipeline, Process Saf. Environ. Protect. 111 (2017) 292–299 ([CrossRef]).

[4] Y. Song, Q. Zhang, Multiple explosions induced by the deposited dust layer in enclosed pipeline, J. Harzard. Mater. 371 (2019) 423–432 ([CrossRef]).

[5] https://www.propublica.org/article/pipelines-explained-how-safe-are-americas-2.5-million-miles-of-pipelines (accessed on March 21,2021) [5].

[6] G. He, Y. Liang, Y. Li, M. Wu, L. Sun, C. Xie, F. Li, A method for simulating the entire leaking process and calculating the liquid leakage volume of a damaged pressurized pipeline, J. Hazard Mater. 332 (2017) 19, 13. [CrossRef].

[7] X. Li, G. Chen, R. Zhang, H. Zhu, J. Fu, Simulation and assessment of underwater gas release and dispersion from subsea gas pipelines, Process Saf. Environ. Protect. 119 (2018) 46–57 ([CrossRef]).

[8] R. Cramer, D. Shaw, R. Tulalian, P. Angelo, M. Stuijvenberg, Detecting and correcting pipeline leaks before they become a big problem, Mar. Technol. Soc. J. 49 (2014) 31–46 ([CrossRef]).

[9] R. Xiao, Q. Hu, J. Li, Leak detection of gas pipelines using acoustic signals based on wavelet transform and support vector machine, Measurement 146 (2019) 479–489 ([CrossRef]).

[10] S. Zhu, Z. Li, S. Zhang, L. Liang, H. Zhang, Natural gas pipeline valve leakage rate estimation via factor cluster analysis of acoustic emissions, Measurement 125 (2018) 48–55 ([CrossRef]).

[11] S. Li, Y. Song, G. Zhou, Leak detection of water distribution pipeline subject to failure of socket joint based on acoustic emission and pattern recognition, Measurement 115 (2018) 39–44 ([CrossRef]).

[12] W. Na, H. Lee, Experimental investigation for an isolation technique on conducting the eletromechanical impedance method in high-temperature pipeline facilities, J. Sound Vib. 383 (2016) 210–220 ([CrossRef]).

[13] M. Kareem, A. Alrasheedy, A. Gafaar, Compensated mass balance method for oil pipeline leakage detection using SCADA, Int. J. Comput. Sci. Secur. 9 (6) (2015) 293–302 ([CrossRef]).

[14] C. Dairo, A method to obtain precise determinations of relative humidity using thin film capacitive sensors under normal or extreme humidity conditions, J. Cult. Herit. 37 (2019) 166–169 ([CrossRef]).

[15] https://oilgas.standards.dnvgl.com/download/dnvgl-rp-f302-offshore-leak-detection((accessed on March 21,2021) [14].

[16] https://rules.dnvgl.com/docs/pdf/DNV/codes/docs/2010-04/RP-F302.pdf(accessed on March 21,2021))[15].

[17] J. Bohorquez, B. Alexander, R. Angus, M. Simpson, F. Martin, M. Lambert, Leak detection and topology identification in pipelines using fluid transients and artficial neural networks, J. Water Resour. Plann. Manag. 146 (6) (2020) ([CrossRef]).

[18] A. Abdulshaheed, F. Mustapha, A. Ghavamian, A pressure-based method for monitoring leaks in a pipe distribution system: a Review, Renew. Sustain. Energy Rev. 69 (2017) 902–911. ISSN 1364-0321.

[19] A.Y. Maidala, A. O, O. E.G, S.G. O, A, Design of a pipeline leakage detection system, Int. J. Adv. Eng. Res. Sci. 4 (2017) 103–110, https://doi.org/10.22161/ijaers.4.5.17.

[20] K.E. Abhulimen, A.A. Susu, Liquid pipeline leak detection system: model development and numerical simulation, Chem. Eng. J. 97 (2004) 47–67, https://doi.org/10.1016/S1385-8947(03)00098-6.

[21] K. Fojtášek, L. Dvořák, L. Krabica, Comparison and mathematical modelling of leakage tests, EPJ Web Conf. 213 (2019), 02019, https://doi.org/10.1051/epjconf/201921302019.